Ultrasonic Laboratory Study of Full Waveform Acoustic Logs in Boreholes with Fractures

by

Fatih Guler and M. N. Toksöz

Earth Resources Laboratory
Department of Earth, Atmospheric, and Planetary Sciences
Massachusetts Institute of Technology
Cambridge, MA 02139

ABSTRACT

A set of ultrasonic experiments was carried out to determine the effects of horizontal and vertical fractures on full waveform acoustic logs. Boreholes of 1 cm diameter were drilled in aluminum blocks. Measurements were made with horizontal fractures of 0.05 mm, 1.0 mm, 2.5 mm, and 4.5 mm width and a vertical fracture of 1.0 mm width. The horizontal fractures of even the smallest thickness significantly attenuate the P, S, and pseudo-Rayleigh waves. The Stoneley waves are the least attenuated, and attenuation increases with increasing fracture width. The vertical fracture attenuates Stoneley waves most significantly. Both scattering and fluid flow play a role in attenuation. The results may qualitatively be extended to inclined open fractures, where we expect strong attenuation of P and S waves and moderate attenuation of Stoneley waves.

INTRODUCTION

Laboratory modeling of acoustic wave propagation in a borehole complements the theoretical studies for the understanding and intepretation of field data. In this paper we describe the ultrasonic experimental results of the effects of horizontal and vertical fractures on full waveform acoustic logs.

Since there are only limited finite difference models for horizontal fractures (Stephen,

1986) and none for vertical fractures, the ultrasonic models do provide the primary basis for understanding effects of such fractures on full waveform acoustic logs, and for interpreting well data from fractured formations.

There are very few papers on laboratory study of full waveform acoustic logs in a borehole (Chen, 1982; Lakey, 1985; Shortt, 1986). None of these addresses the problem of vertical fractures. One difficulty of laboratory work is the complexity of experiments, particularly adequate scaling of physical dimensions and wavelengths. The second problem arises on the complexity of waveform microseismograms which require sophisticated field data for the identification of wave types and interpretation of the results.

EXPERIMENTAL METHOD

In this study we use wavelength scaling for determining physical dimensions of the model, including the borehole radius. The frequency response of the source-receiver transducers covers a range of 100 kHz - 600 kHz. The modeling material is aluminum with velocity and density corresponding to those of a hard limestone or dolomite (Table I). The borehole diameter is 1 cm. With these specifications our model corresponds to a 5–30 kHz frequency band in the field with a 20 cm (8") diameter borehole in dense carbonate. Thus the model is reasonably analogous to studying fractures in low-porosity, low-permeability carbonates, cherts or crystalline rocks. The borehole source and receiver are piezoelectric hydrophones. The fundamental frequency of the source used is about 120 kHz and the diameter is 9.65 mm. The receiver response is flat ($\pm$ 3 dB) between 1 kHz and 600 kHz and it has a diameter of 6.35 mm (0.25 in) (Figure 1). The actual piezoelectric elements are smaller than the cited diameters, which include the rubber protective layer around the elements.

The data are collected with a fixed source and a moving receiver. This method mainly helps to identify waves by their move-out. Aluminum blocks are placed in a water tank and the tank is filled with tap water. Even though the experiments are repeatable, generally for a given setup all waveforms are collected within a relatively short-time period of several hours. This assures fixed temperature and environmental conditions for each experiment.

Two identical, but separate, aluminum cylinders with diameter 20 cm (8") and length 30 cm (12") are used for horizontal and vertical fracture experiments. Each cylinder is center drilled and reamed with a 25/64" reamer to produce a smooth 1 cm diameter borehole. Full waveform experiments are performed before fractures are introduced. For horizontal fracture experiments one aluminum block is cut in two, normal to the borehole axis, with one segment 13 cm (5.25") long and the other 11.5 cm (4.5") long. The surfaces are polished to ensure flatness.
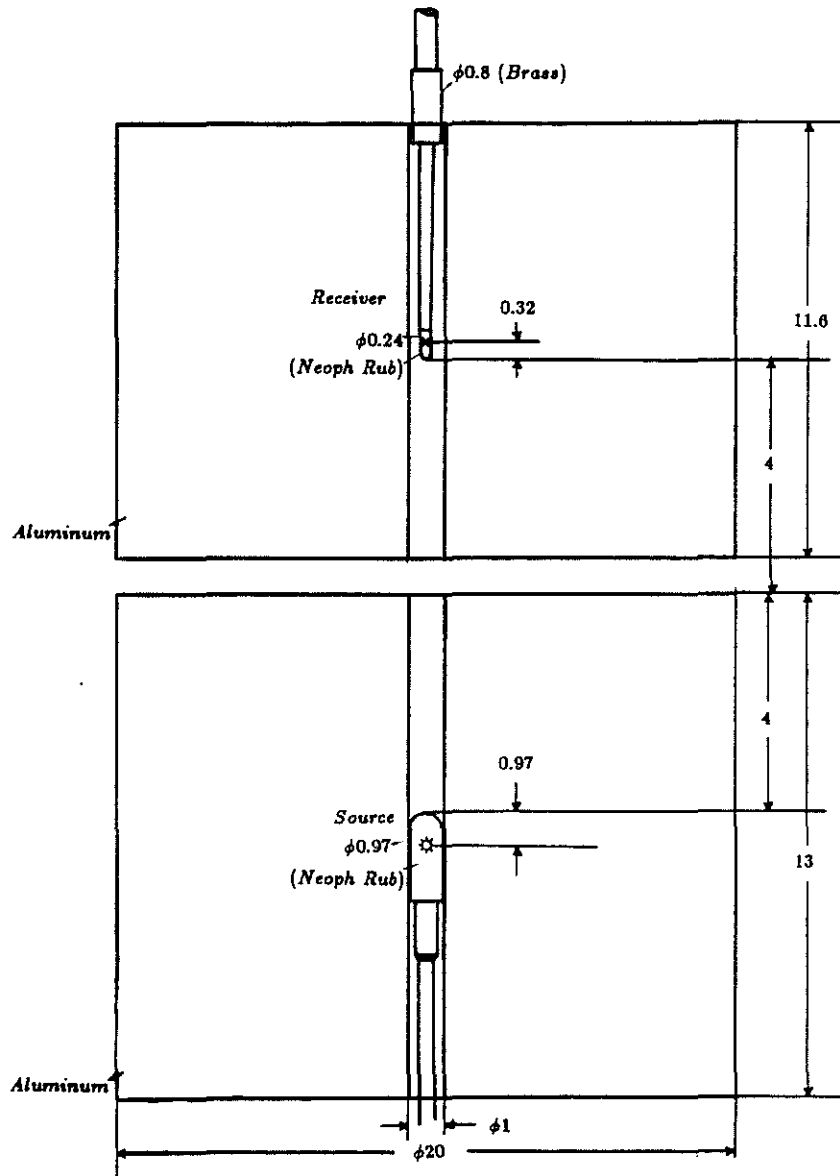
Figure 1: The physical dimensions (in cm) of the setup.

These two pieces are used to simulate a horizontal fracture. The fracture width is varied by 3 shims which are placed between the blocks, 120° apart, and far from the borehole. The shims have 0.5, 1.0, 2.5, and 4.5 mm thicknesses to obtain different fracture widths. The z-axis alignment of the boreholes in the two separate blocks is assured by moving a 9.9 mm diameter, 35 mm long guide inside the boreholes.

The source is placed 40 mm below the fracture and the receiver is moved from 0 mm to 86 mm in 2 mm steps, 0 mm being the location of the tip of the source. The receiver is attached to a mechanism that continuously moves up and down by turning a screw. The assembly is clamped to the top of the water tank. The aluminum blocks are leveled to ensure parallelism between the receiver and borehole axis. The tank is filled with water and the data are collected after waiting two days to let the air bubbles disappear and the water to reach room temperature.

The source is excited by a high voltage pulse generator (VELONEX, 350) with settings of 400 V and a 0.8 μsec pulse. The receiver output is amplified by a 0–5 MHz bandwidth DC amplifier (HP, 465 A) with 20 dB gain. Data are recorded by a transient capture digital oscilloscope (Data Precision, D6000) at 400 nsec sampling rate for a period of 409.6 μsec. Each waveform is averaged in real time for 10 traces and stored (Data Precision, 681) on IBM formatted floppy disks. The collected data are transferred via an IBM PC-AT to a VAX 11/780 for further processing (Figure 2). The acoustical properties of the measurement media are given in Table I.

Table I. Acoustic Parameters of Materials Used in the Experiments

Material	Velocity km/sec		Density gm/cm^3	Poisson's Ratio
	v_p	v_s	ρ	ν
Aluminum	6.10	3.10	2.70	0.34
Water	1.48		1.00	0.50
Neophrene Rubber	1.60	0.10	1.33	0.49

The vertical fracture is produced by sawing the second block into two-halves from the top to a depth of 12 cm (4.75"). The bottom half of the block remained intact to serve as the reference borehole. The width of the vertical fracture is 1.0 mm. The measurements are carried out using exactly the same procedure for the horizontal fracture case. The source is placed 4 cm below the fracture and the receiver moved at 2 mm increments, to log first the unfractured borehole, and then the fractured borehole.
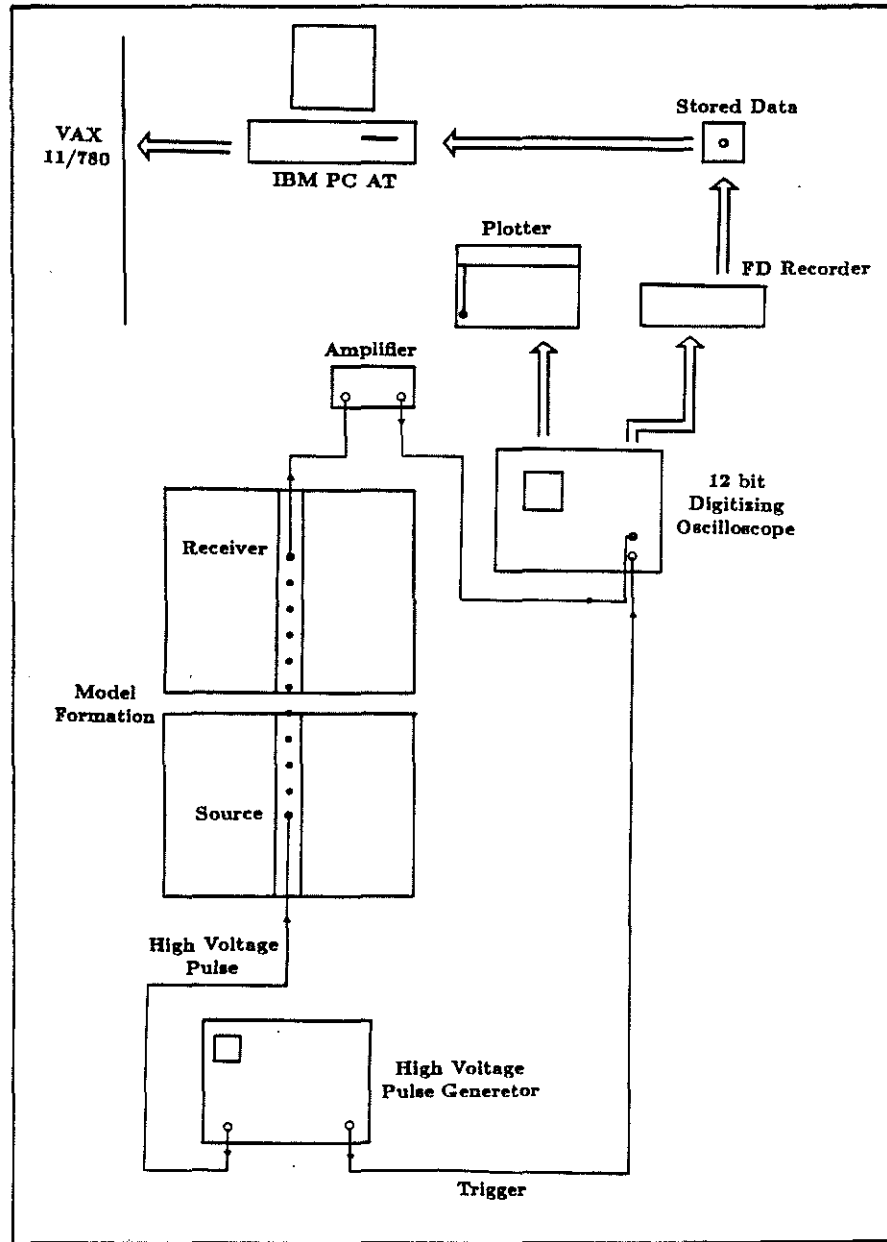
Figure 2: Flow diagram of data acquisition setup.

EXPERIMENTAL RESULTS

Horizontal Fracture

The experimental full waveform acoustic logs are shown as a function of increasing distance between the source and receiver for both horizontal and vertical fracture experiments. In addition to broad-band microseismograms, frequency-wavenumber plots are calculated in order to identify the different modes of pseudo-Rayleigh and Stoneley waves. Then the Stoneley waves are separated, by low-pass filtering, in order to demonstrate the effects of fractures on these waves. Finally, the attenuation of different wave types due to fractures is shown by plotting the amplitude ratios of transmitted to incident waves.

The horizontal fracture data are shown first. Figures 3a,b,c,d are the broad-band microseismograms for source receiver spacing of 2 mm to 86 mm. The fracture is at 36.5 mm and marked on each figure. Figure 3a represents the thinnest fracture with only a thin layer of water ($\approx$ 0.05 mm) separating the two blocks. As fracture width increases (Figures 3c,d) it becomes clear that P, S, and the faster branches of the pseudo-Rayleigh wave train disappear. The high frequency late arriving phase (those waves arriving after the Stoneley wave) are the Airy phases of the pseudo-Rayleigh waves. There is also evidence that there is more than one mode of pseudo-Rayleigh wave.

The identification of different modes can best be done by calculating the frequency-wavenumber spectra. Figures 4a,b show the f-k spectra for the 1.0 mm fracture width. The top figure (4a) is when the receiver is above the fracture while the source is below, thus representing the transmitted waves. The bottom figure (4b) is the case in which both the source and the receiver are below the fracture. The lowest frequency waves are the Stoneley waves, and both the direct waves and those reflected back from the fracture are obvious. Several modes of pseudo-Rayleigh waves are also obvious. Backscattered waves complicate the figure. For the transmitted case (Figure 4a) one sees the reduced amplitudes of the Stoneley wave and of the lower frequency (fundamental mode) pseudo-Rayleigh wave. At higher frequencies there are five modes of the pseudo-Rayleigh wave, some of which may be produced by the scattering of the Stoneley wave or the fundamental mode of the pseudo-Rayleigh wave into higher modes.

The low-pass filtered seismograms show the Stoneley waves in Figure 5 for four fracture widths: 0.05, 1.0, 2.5, 4.5 mm. Note that as fracture width increases, the attenuation of the Stoneley wave across the fracture increases. Stoneley waves reflected from the fracture are especially obvious (upgoing waves) in the bottom two figures. The attenuation of different waves as they travel across the fracture is shown in Figure 6. The amplitude ratio is the peak-to-peak ratio of the amplitudes of the transmitted to

incident wave, except the pseudo-Rayleigh wave (which is RMS amplitude). If there were no fracture (fracture width = 0.0 mm) these values would be unity. Of the four waves, even the thinnest fracture (0.05 mm wide) almost completely attenuates the S waves. P-wave attenuation is also substantial especially when fracture width is greater than 0.05 mm. For the pseudo-Rayleigh waves, RMS amplitudes are plotted since this is a dispersed wave train. Attenuation is significant. The wave attenuated the least while crossing the fracture is the Stoneley. For horizontal fractures, Figure 6 can serve as a good qualitative guide for identifying fractures from relative attenuation of different phases of the full waveform acoustic logs.

Accurate determination of fracture width from attenuation measured on the model is difficult to scale to lower frequencies in the real earth case. Not all the phenomena responsible for attenuation (scattering to other waves, fluid flow) obey the linear wavelength scaling. As a result, the ultrasonic laboratory measurements can only serve as a qualitative guide for interpreting the field data. The quantification requires either large scale physical models or numerical theoretical models that are confirmed by the laboratory data.

Vertical Fracture

The broad-band microseismograms of full waveform acoustic logs for a vertical fracture that is 1.0 mm wide are shown in Figure 7. The fracture starts at 36.5 mm and extends to 86 mm (as shown on the right of the figures). The microseismograms show relatively little or no attenuation of P, S, and pseudo-Rayleigh waves, but an attenuation of Stoneley waves.

The frequency-wavenumber plots shown in Figure 8a and b are quite illustrative. The top figure (8b) represents the fractured section of the borehole, where there are a number of pseudo-Rayleigh modes dominant at the high frequencies. In the unfractured zone (8b) the Stoneley waves dominate over the pseudo-Rayleigh modes.

The attenuation of Stoneley waves by a vertical fracture is illustrated in Figure 9. Note that amplitudes decreases with increasing propagation along the fracture.

Figure 10 is the actual amplitudes of the waves versus the increasing source-receiver separation. All amplitudes are peak-to-peak except for the pseudo-Rayleigh waves, where the RMS amplitudes are used. No corrections have been made to P- and S-wave amplitudes to account for geometric spreading. It is clear that P and S waves show little or no attenuation due to the vertical fracture. The pseudo-Rayleigh wave (pR) shows an increase in amplitude in the fractured zone due to the energy scattering from the Stoneley wave to the pseudo-Rayleigh wave. The Stoneley wave shows rapid attenuation

due to the fracture because of leakage of energy into the fracture. Thus the attenuation properties for a vertical fracture are quite different from those of horizontal fractures.

CONCLUSIONS

The ultrasonic laboratory experiments for full waveform acoustic log propagation in a borehole with horizontal and vertical fractures provide some insights for the identification of such fractures in the field data. The model experiments represent some ideal geometries, in terms of perfectly horizontal and vertical fractures.

We expect that inclined fractures will affect the P and S waves in a way similar to horizontal fractures. For the guided Stoneley and pseudo-Rayleigh waves the attenuation may fall between those of purely horizontal and purely vertical fractures.

The experimental results apply only to "hard" formations because the energy distribution and coupling changes (especially for Stoneley waves) with changing shear modulus of the medium. Both aluminum and borehole fluid (water) have very high Q_s. As a result model experiments show the fracture effects on amplitudes without the effects that would arise from intrinsic attenuation. On the other hand, since the ultrasonic waves have frequencies higher by an order of magnitude than those of full waveform acoustic logging field tools, attenuation due to fluid flow from the borehole into fractures is less in the laboratory data.

In the light of these nonscalable differences between the laboratory and field conditions, it is prudent to weigh the laboratory results appropriately when comparing them with the field data.

ACKNOWLEDGEMENTS

REFERENCES

Chen, S. T., 1982, The full acoustic wave train in a laboratory model of a borehole; Geophysics, 47, 1512-1520.

Lakey, K. G., 1985, Physical modelling of the full acoustic wave train in a borehole with a perpendicular fracture; M.S. Thesis, Washington State University, Pullman, Washington.

Shortt, E. R., 1986, Laboratory borehole model; M.I.T. Full Waveform Acoustic Logging Consortium Annual Report.

Stephen, R. A., 1986, Synthetic acoustic logs over bed boundaries and horizontal fissures; M.I.T. Full Waveform Acoustic Logging Consortium Annual Report.
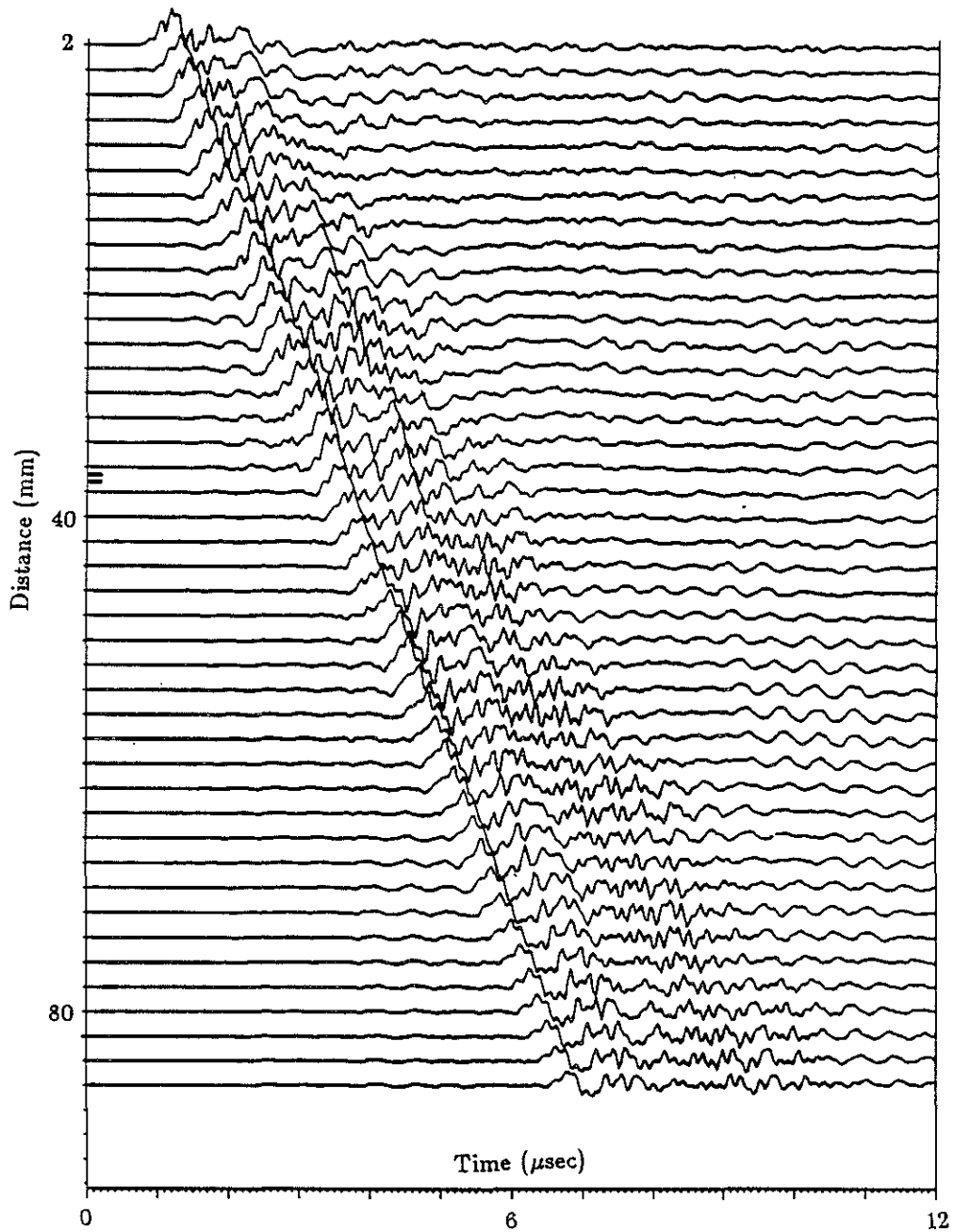
Figure 3: (a) Broad-band microseismograms of the full waveform acoustic logs as a function of increasing source-receiver separation across a horizontal fracture indicated on left hand axis near 38 mm distance; fracture width is about 0.05 mm.
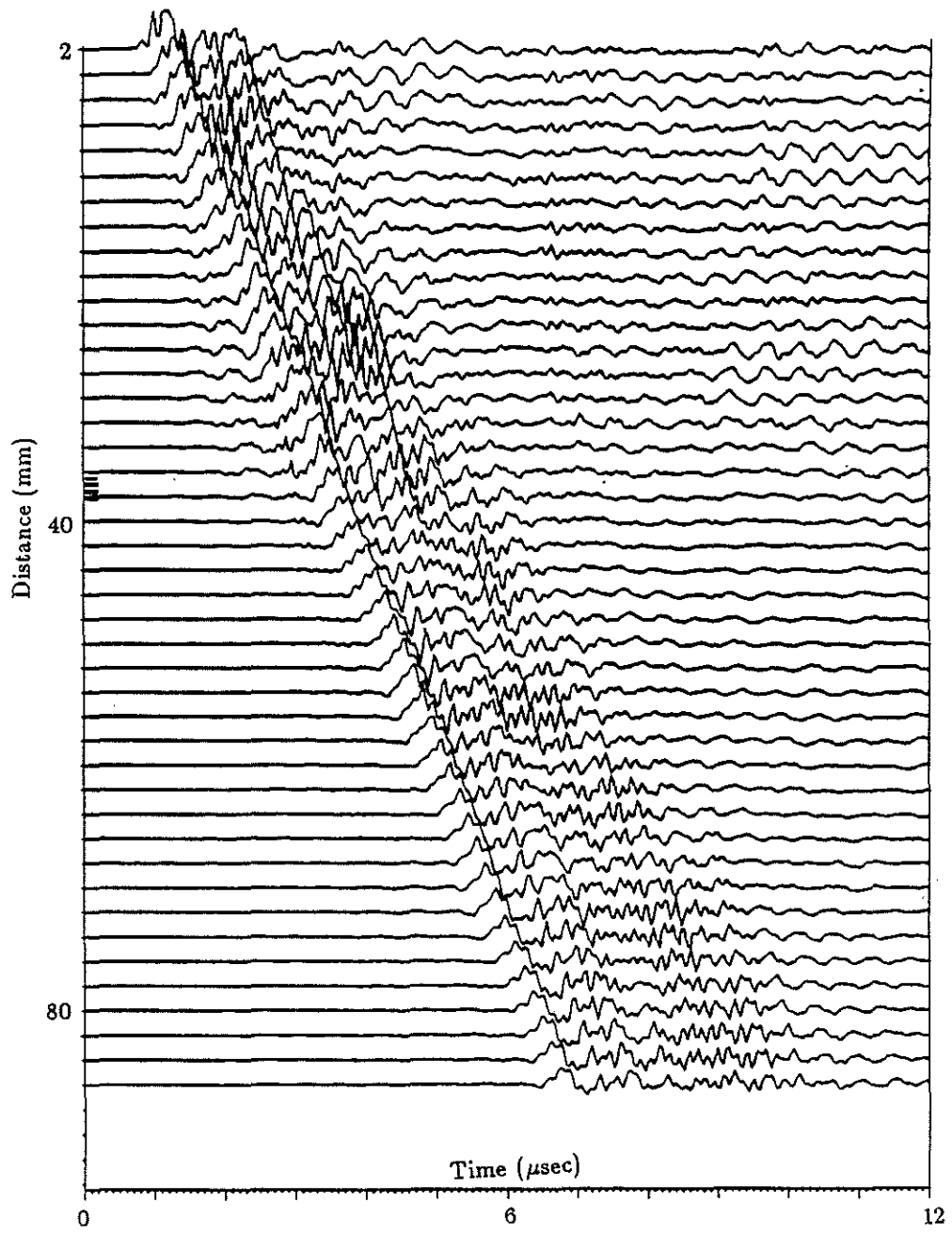
Figure 3: (b) Same as Figure 3a except with a fracture width of 1.0 mm.
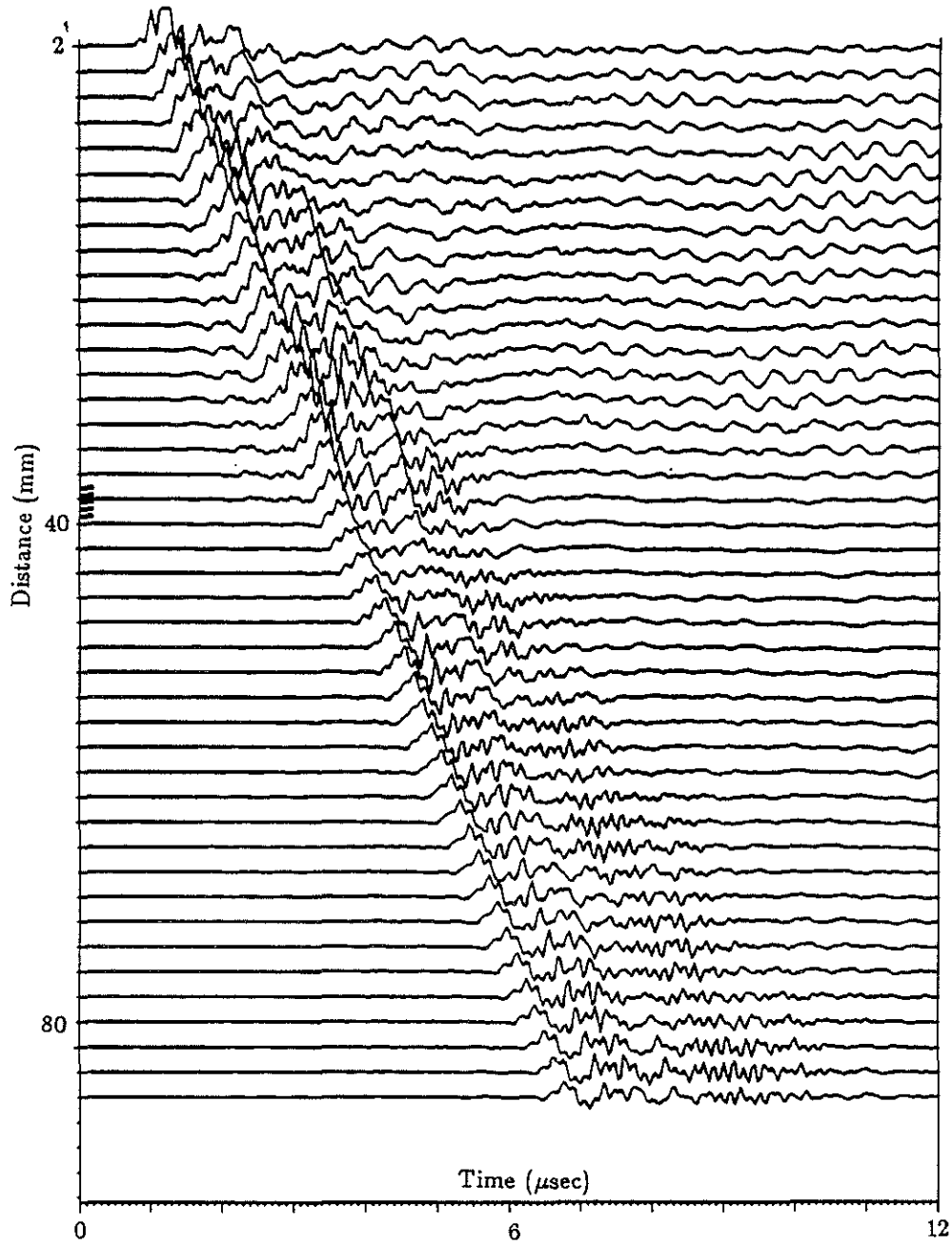
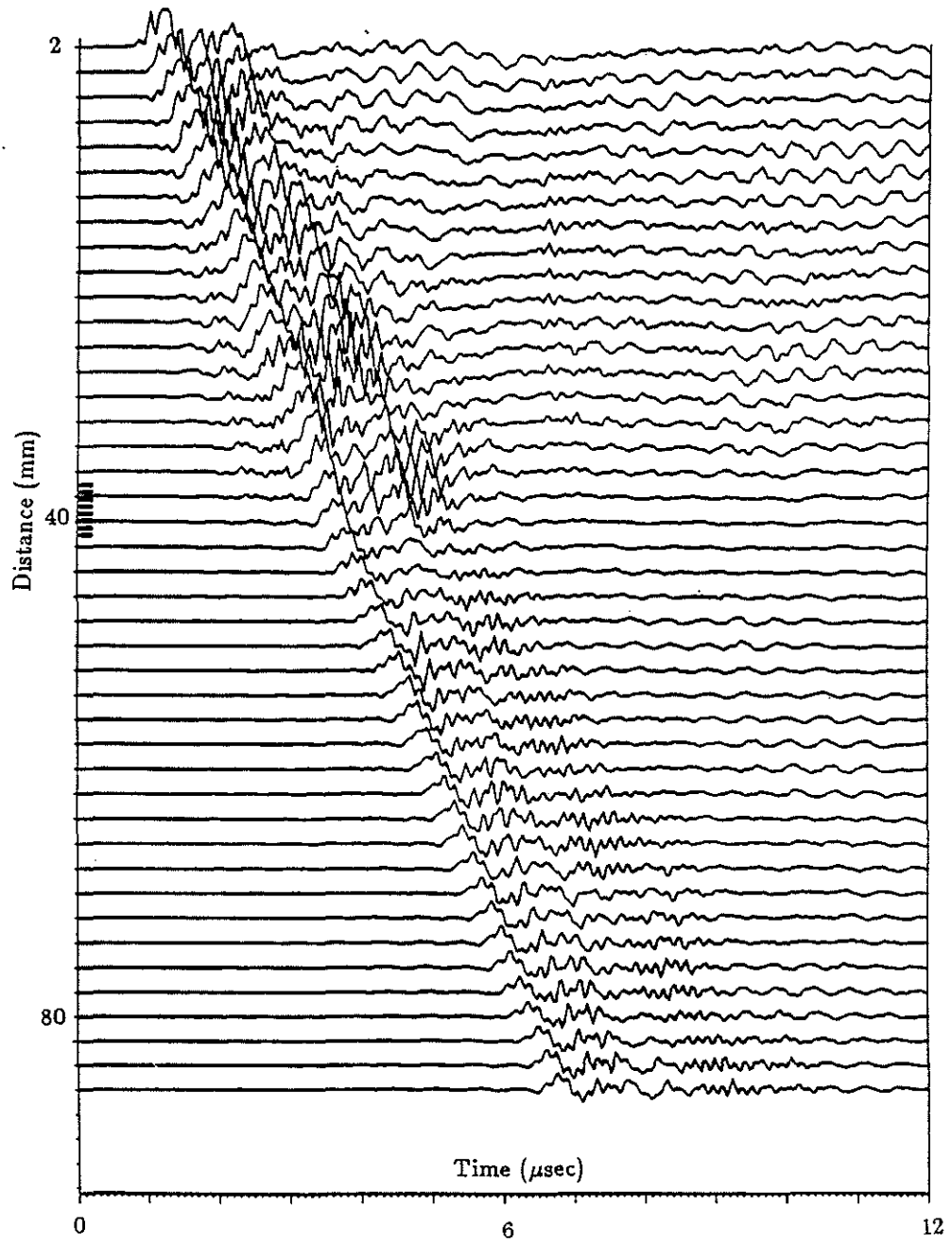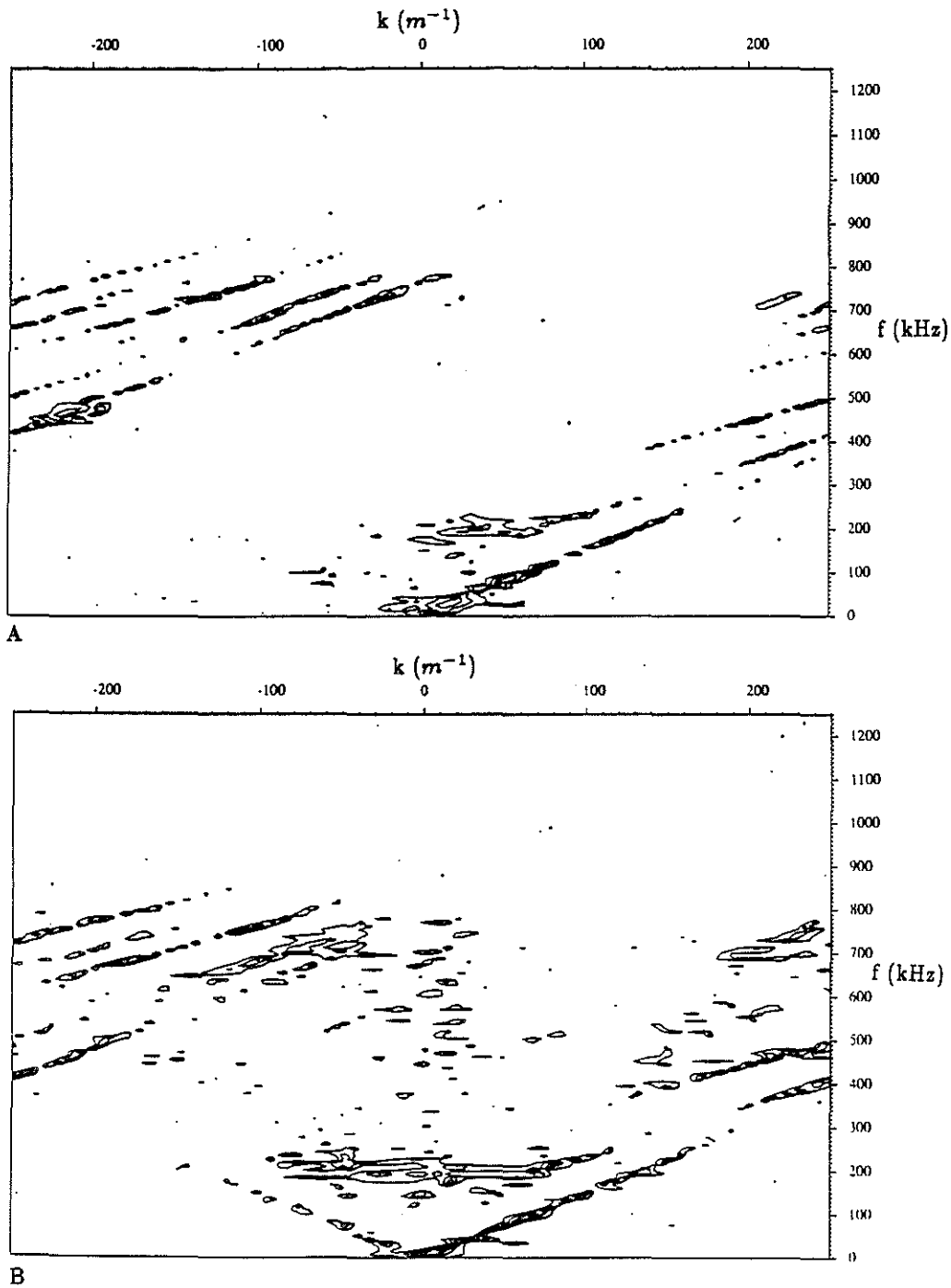Figure 3: (c) Same as Figure 3a except with a fracture width of 2.5 mm.

Figure 3: (d) Same as Figure 3a except with a fracture width of 4.5 mm.

Guler and Toksöz

Figure 4: Frequency-wavenumber (f-k) diagrams of full waveform acoustic waves in a borehole with a 1.0 mm horizontal fracture. Top (a) is for waves transmitted across the fracture. Bottom (b) is for both source and receiver below the fracture.
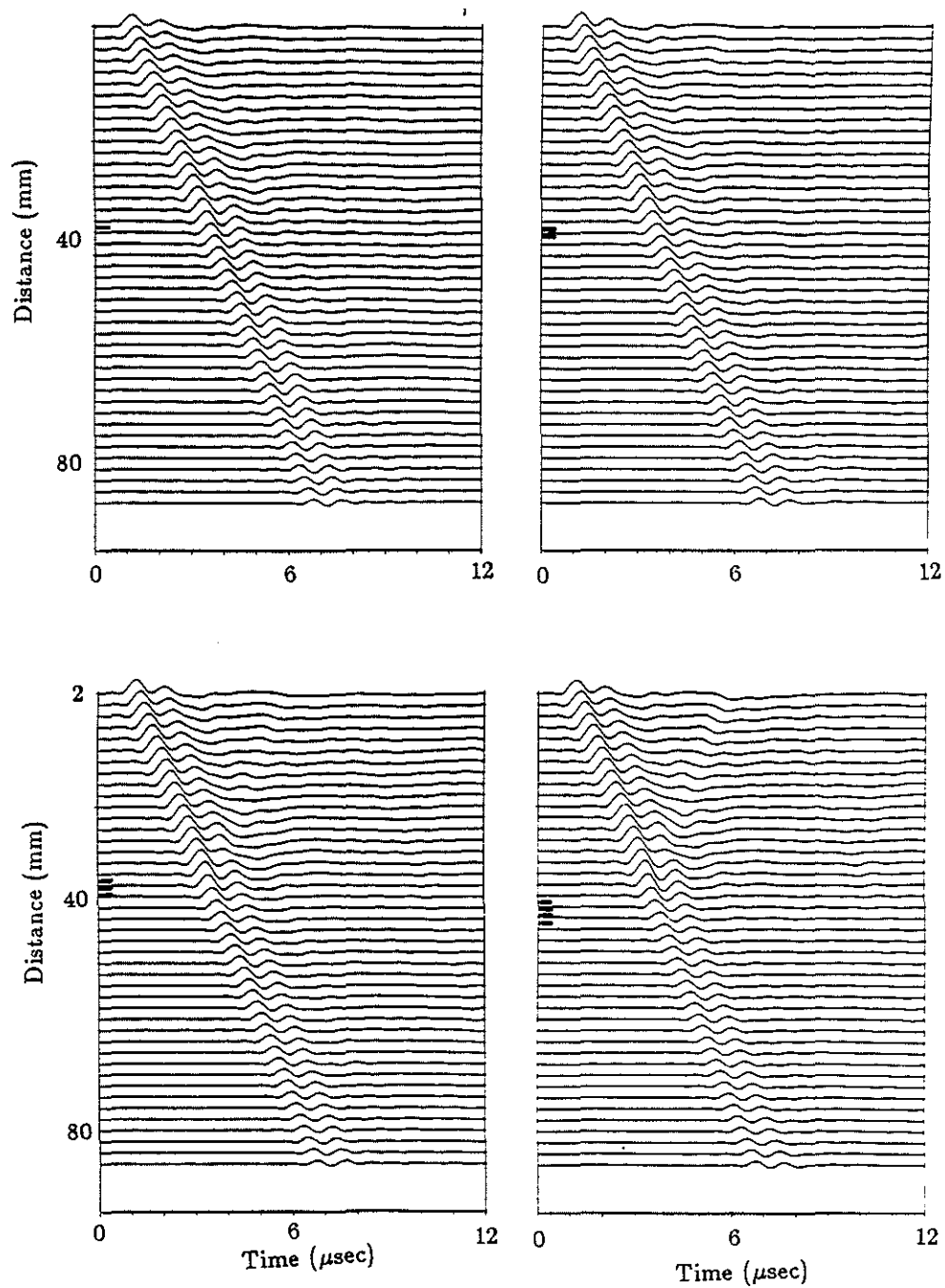
Figure 5: Low frequency filtered microseismograms showing Stoneley waves crossing horizontal fractures. Fracture widths increase from about 0.05 mm (top left) to 4.5 mm (bottom right). Fractures are indicated on the left hand axis at 36.5 mm.
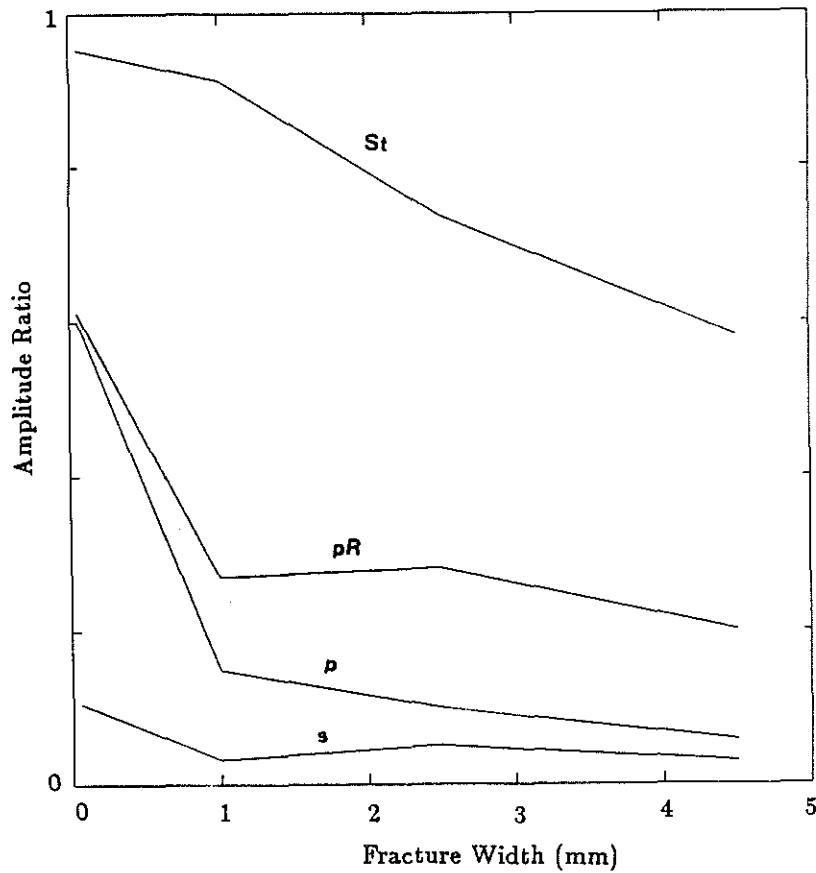
Figure 6: Amplitude ratios of transmitted to incident waves across horizontal fractures as a function of fracture width. Amplitudes are peak-to-peak maximum amplitudes except for the highly dispersed pseudo-Rayleigh wave (pR) where average RMS amplitudes are used. Note that the S (s) wave is the most attenuated by the horizontal fracture while the Stoneley wave (St) attenuated the least. If there were no fracture (FW = 0.0) all values would be 1.0.
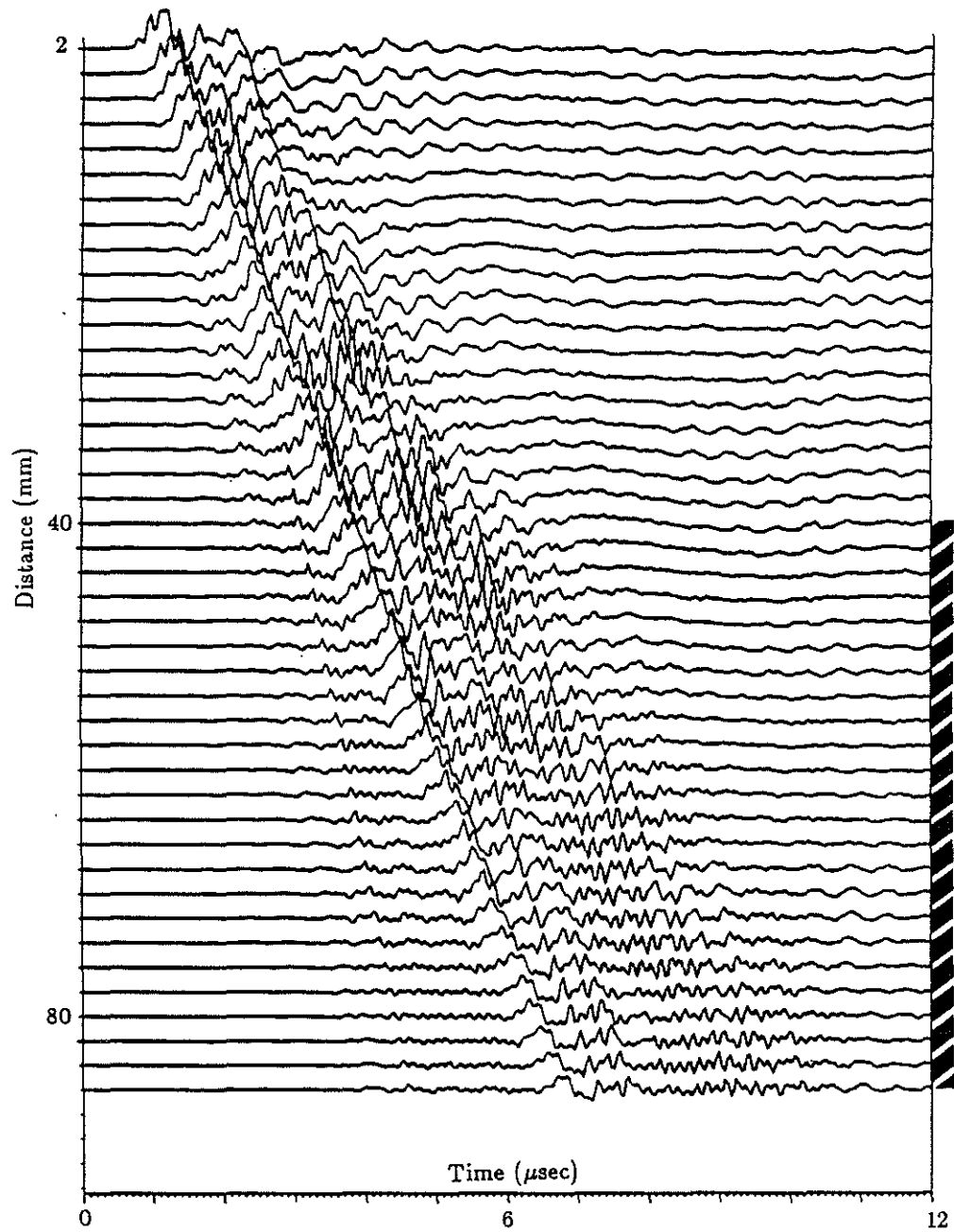
Figure 7: Broad-band microseismograms of the full waveform acoustic logs as a function of increasing source-receiver separation across a vertical fracture extending from 38 mm to 86 mm indicated on right hand axis. The fracture width is 1.0 mm.
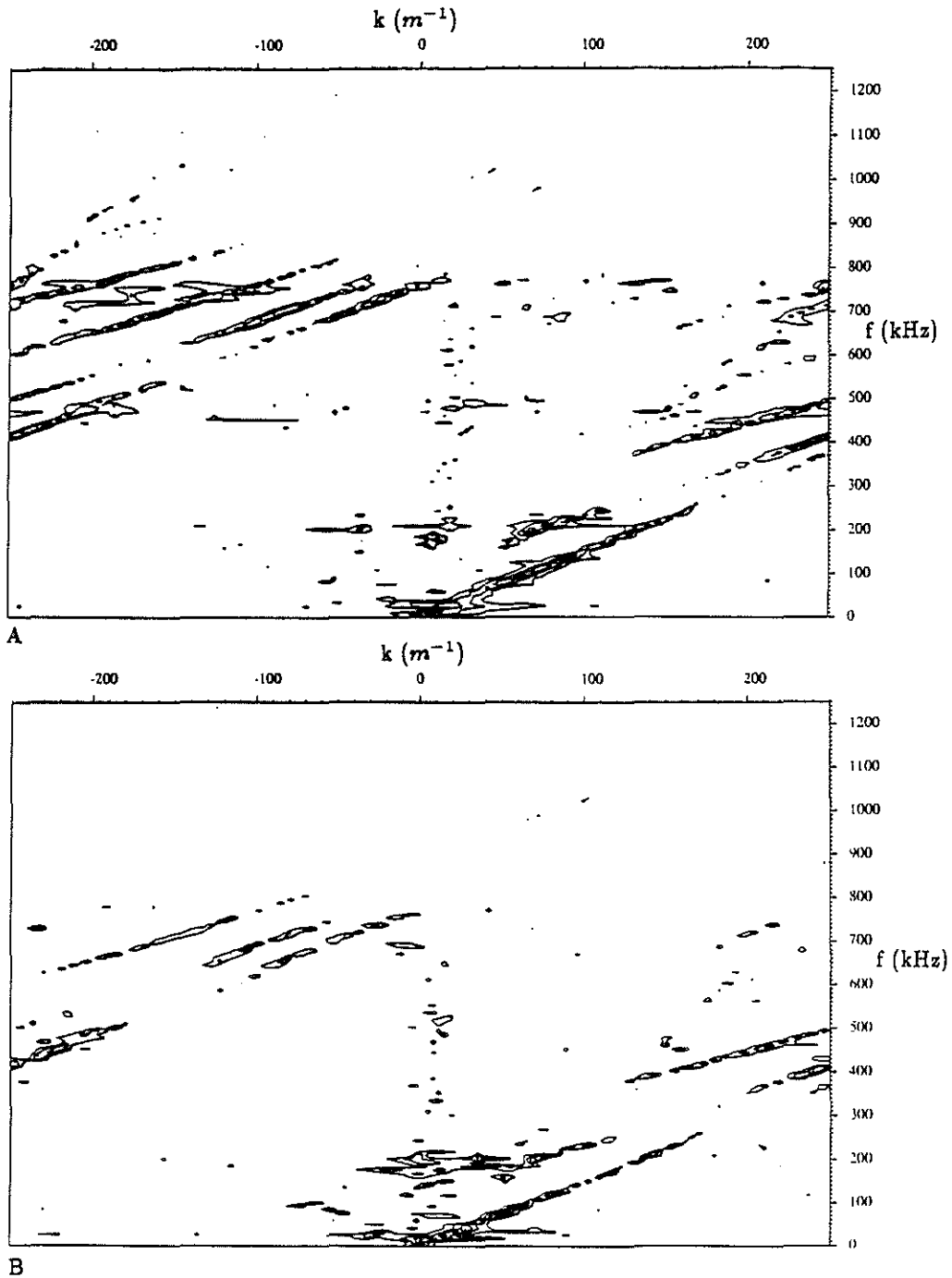
Guler and Toksöz

k (m^{-1})

Figure 8: Frequency-wavenumber (f-k) diagrams of full waveform acoustic waves in a borehole with a 1.0 mm wide vertical fracture. Top (a) is for waves transmitted along the fracture. Bottom (b) is for when both source and receiver are below the fracture.
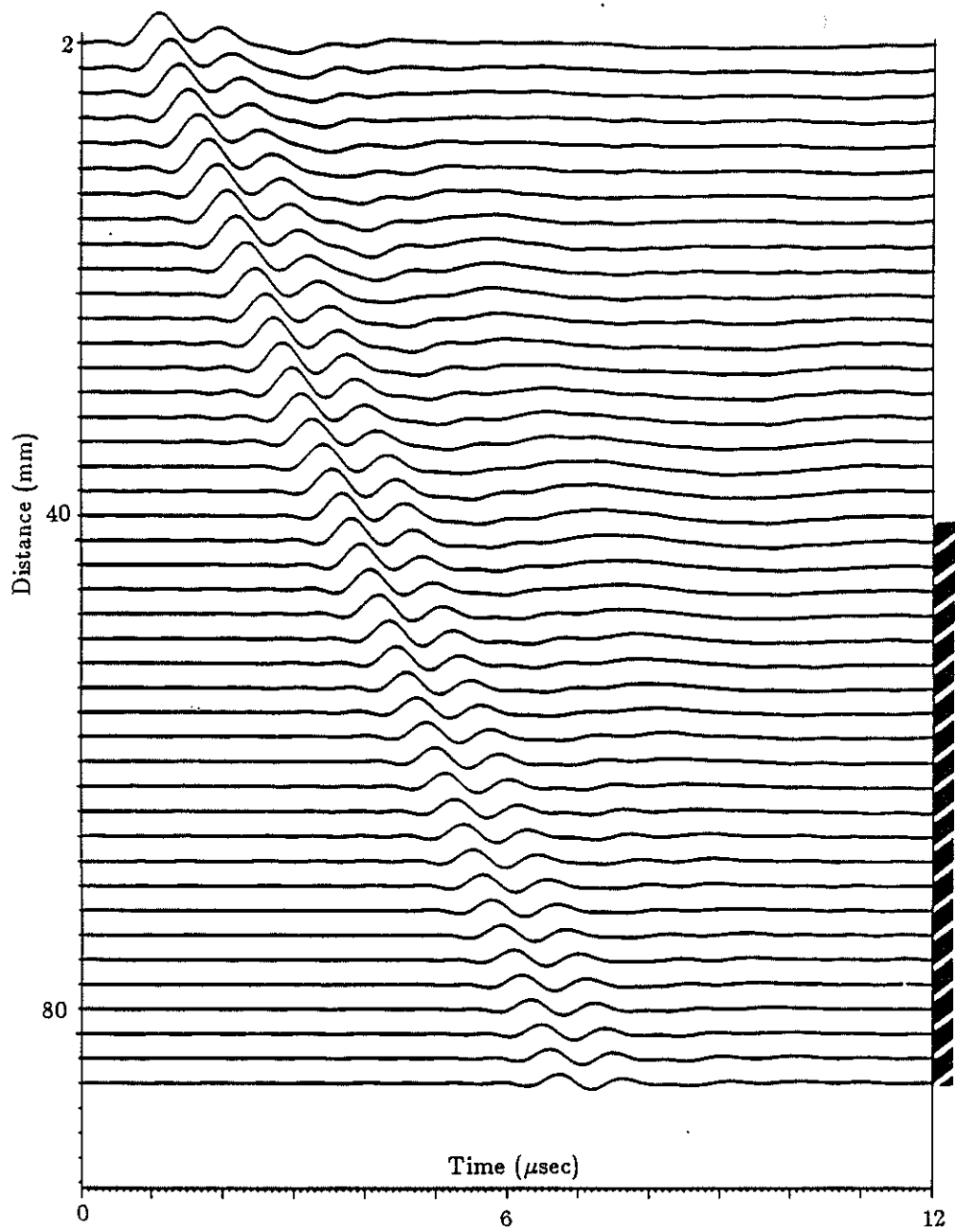
Figure 9: Low frequency filtered microseismograms showing the Stoneley waves in a vertical fracture extending from 38 mm to 86 mm indicated on right hand axis. The fracture width is 1.0 mm.
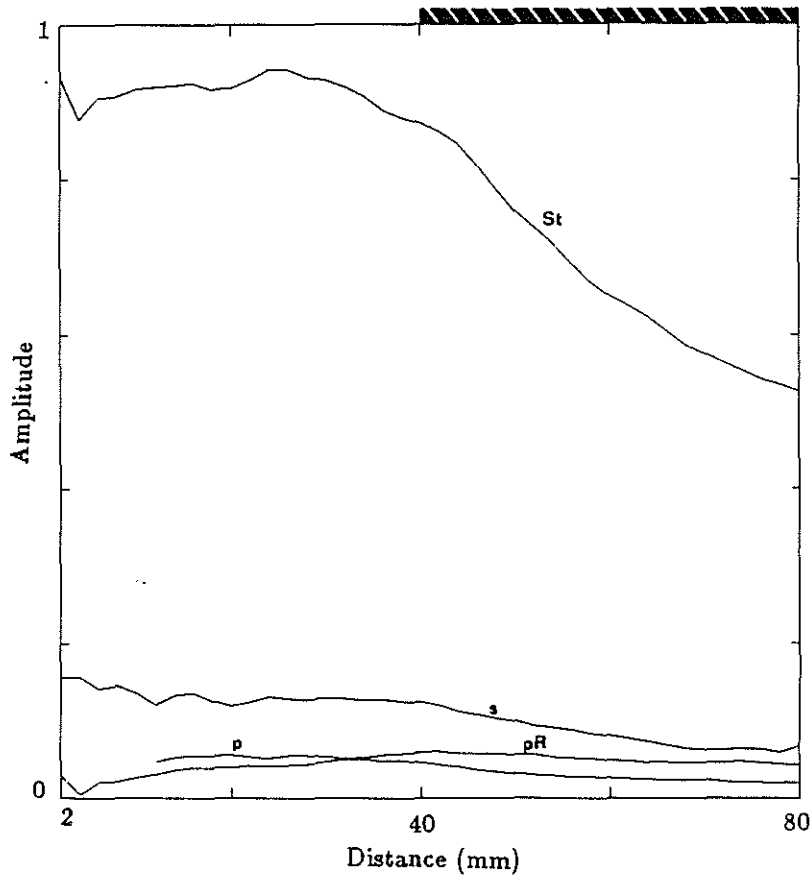
Figure 10: Actual amplitudes of the waves versus source-receiver separation in a vertical fracture extending from 38 mm to 86 mm indicated on right hand axis. The fracture width is 1.0 mm. Amplitudes are peak-to-peak maximum amplitudes except for the pseudo-Rayleigh waves which are RMS amplitudes. Note that the major difference on amplitude occurs in the Stoneley waves (St) which decrease along the fracture. The pseudo-Rayleigh wave (pR) amplitudes increase in the fractured zone due to energy scattering from the Stoneley waves.